Document Header Id #: 102656
Sponsor: PRATT & WHITNEY AIRCRAFT/
Award Document: DO Contract #: 20195 / 19
Project Director(s): JOHNSON WILLIAM STEVEN Contract thru: GTRC
Unit: MSE
Initiation Date: 01-JAN-2006 Termination Perf Date: 31-DEC-2006 Termination Rpts Date: 31-DEC-2006
Project Title: 3-D FRACTURE CRITERION USAGE/VADIATION

Rev No (1)	Description of Deliverable	Deliv Id No (2)	Period Covered		Due Date to Sponsor (3)	Copies Reqd	Date Mailed (4)
	FINAL REPORT	1	01-JAN-2006	31-DEC-2006	31-DEC-2006	1	22-JAN-2007
	DATABASE OF FULLY 3-D MIXED MODE CRACK PATHS	2				1	
	FINITE ELEMENT MODELS	3				1	
	QUANTITATIVE ASSESSMENT	4				1	

PLEASE NOTE:
1. An asterisk denotes this deliverable was changed or added by this mod.
2. The Deliverable Id No will remain associated with its originally assigned deliverable for the duration of the project. Modifications to the project will no longer cause this number to be sequentially renumbered.
3. Blanks in 'Due Date to Sponsor' indicate 'as appropriate' or 'as required'.
4. Blanks in 'Date Mailed' indicate that neither delivery nor notification of delivery has been accomplished through OSP/CSD.

Prepare reports in accordance with:
The complete title of Data Del ID #3 is "Finite element models of 3-D crack paths and characterization of crack driving forces" and the complete title of Data Del. ID #4 is "Quantitative assessment of current and proposed advanced 3-D crack path selection criteria".

1026086
1

Larissa Woods

From: rusty.edwards@mse.gatech.edu
Sent: Thursday, January 25, 2007 11:52 AM
To: ocareports
Subject: Project 1806C92 - Pratt & Whitney Final Report

pratt-yr1.pdf (1 MB)

I am attaching a copy of the final report that Dr. Johnson sent to Pratt & Whitney on 01/22/07. Thank you, Rusty <<pratt-yr1.pdf>>

Rusty Edwards
MSE Financial Manager
(404) 894-5791

JAN 25 2007
2:30pm

LW
1/25

3-D Fracture Criterion Usage/Validation Year 1 Report

P&W Contract 20195FW (Task #19)
GT Project #E18-C92

Submitted to

Dr. Richard Pettit
Technical Monitor
Pratt & Whitney Aircraft Engines
400 Main St.
East Hartford, CT 06108
richard.pettit@pw.utc.com

Submitted by

Dr. W. Steven Johnson, Principal Investigator
Shelby Highsmith, Jr., Graduate Researcher
School of Materials Science & Engineering
Georgia Institute of Technology
Atlanta, GA 30332-0245
steve.johnson@mse.gatech.edu

January 2007

Executive Summary

Understanding of crack path selection under mixed mode loading is necessary for fracture-critical components which experience complex stress states, but the vast majority of mixed mode crack growth research has covered the superposition of only two of the three modes. In light of evidence that significant levels of Mode II loading can in some cases lead to a modal transition from normal to shear mode crack growth, further study of shear mode loading effect incorporating all three modes is desired. To that end, two new tension-torsion crack growth specimen designs have been developed and analyzed using FRANC3D boundary element modeling software, and both are shown to generate significant proportions of shear mode stress intensities. Two modes can be controlled independently of the third for out-of-phase studies, and the internal through-crack round specimen generates a distribution of Mode II stress intensities across the crack front for investigations into critical mixity levels required for modal transition. Closed form stress intensity solutions for both specimens have been developed from several simulations of varying geometry.

In order to validate the numerical analyses of the new specimen designs, several surrogate specimens have been machined from PMMA (plexiglass) for preliminary testing, planned for early 2007. The crack path behavior of PMMA is well understood and thus will be able to confirm baseline predictions of the numerical modeling. Manufacturing delays were encountered in fabrication of titanium specimens for final testing. Preliminary specimens that have been machined do not all meet tolerance requirements for testing, so work has begun on adapting tooling so that they may be tested. Additional specimens are being machined to meet tolerance requirements. Final testing of titanium specimens is planned for Spring 2007.

Contents

1 Introduction

The damage tolerance approach to determining fatigue life limits of fracture-critical components presupposes the existence of flaws in components and calculates the safe usable life before a crack grows to a critical size. Initial work in damage tolerance was based largely on linear elastic fracture mechanics analysis of Mode I loading and crack growth. However, components under stress may have initial or induced flaws in them oriented at any arbitrary angle relative to the nominal stress field that can thus be subject to Mode II and III loading from the outset, or cracks may grow into complex and varying stress fields that alter the stress state at the crack tip. In the application presently of interest, turbine blades are subject to aerodynamically induced vibratory modes including flapping and twisting, which when superimposed on the centrifugal load contribute to three dimensional mode mixity on any crack-like flaws. The influence of these complex loading states on crack growth must be understood for its dual impact on damage tolerance analyses. Not only can mixed mode loading change the crack growth rate compared to simple Mode I loading (for which the most experimental data is available), it also dictates the direction of fatigue crack propagation. In a spatially varying stress field, the crack path dictates the subsequent stress intensity at the crack tip and resulting crack growth rate. Additionally, in cases of high-speed rotating components like turbine engine rotors, the crack path will dictate the size (and thus kinetic energy) of any fractured ligament that may be liberated, setting the case containment requirements. To better understand crack path selection in various materials, experimental data is required for generalized mixed mode loading in which all three crack loading modes occur. A number of specimen designs exist for crack growth testing under 2-D mixed mode conditions using simple uniaxial loading. This paper describes two new tension-torsion specimen designs for three-mode crack loading and presents stress intensity factor results generated from 3-D boundary element element modeling (BEM).

2 Project Background & Objectives

Studies of mixed mode crack growth in two dimensions (Modes I and II) have established some successful criteria for crack path direction, starting with the maximum tangential stress (MTS) criterion developed by Erdogan and Sih [1] in 1963. Subsequent criteria put forth included the maximum strain energy release rate or "Griffith" criterion [2], the minimum strain energy density or S-criterion [3], and the $K_{II} = 0$ criterion [4]. All of these models project nearly the same crack path deflection angle under in-plane mixed mode loading, such that the crack turns to propagate normal to the maximum principal stress (i.e., to continue in Mode I loading). Due to its simplicity and a significant population of supporting data, the MTS criterion is frequently used. This model has been extended to the three-dimensional case by Tian *et al.* [5] and Schollmann *et al.* [6].

Most of the available mixed mode data show the effects of interaction between only two of the three possible loading modes. A very comprehensive mixed mode crack growth literature review published by Qian and Fatemi [7] in 1996 discussed only studies that superimposed one shear mode upon normal crack loading (Modes I and II or I and III). Only a few recent experimental studies have considered the superposition of all three modes at once [8, 9, 10, 11, 12]. Some of the earlier 2-D studies have shown that there can be a significant effect of the in-plane shear Mode II on both the crack growth rate and direction in mixed Mode I and II loading. Hallback and Nilsson [13] and Amstutz *et al.* [14], for example, have observed a crack growth mode transition from normal (Mode I) to shear (Mode II) crack growth in some materials at higher levels of initial Mode II load component, in which the crack follows a path predicted by the maximum shear stress (MSS) criterion. Chao and Liu [15] proposed a failure mechanism map based on the crack tip loading path and competing MTS and MSS criteria, pointing to a modal transition at K_{II}/K_I ratios related to material properties.

Further study of this modal transition and extension of the associated crack growth criteria to three-dimensional stress states is required. As mentioned above, there is very little data on 3-D mixed mode crack growth, and the crack path criteria cited are based upon the MTS criterion so that a transition to MSS-predicted crack paths are not considered. To that end, two new tension-torsion specimen designs have been developed and analyzed to explore different combinations of all three modes of crack tip loading for generalized 3-D mixed mode crack growth. Validation testing on surrogate PMMA specimens proceeded by material characterization tests on titanium alloy Ti-6Al-4V will follow.

3 Project Approach / Statement of Work

3.1 Task 1 - Mechanical Testing

Georgia Tech (GT) will perform tension-torsion fatigue crack growth tests on up to thirty (30) specimens total of up to three (3) design configurations. Specimens will be provided by Pratt & Whitney. Specimen configurations will be designed by Pratt & Whitney in consultation with GT such that the specimens will mate with existing tooling at GT. Tests will be conducted in such a manner as to generate combinations of Mode I, Mode II, and Mode III loading conditions and HCF/LCF interactions as specified by Pratt & Whitney. GT will record mechanical and/or electrical data as appropriate to monitor fatigue crack growth rate. The primary data deliverable from testing will be post-test quantitative fractography to characterize crack path direction in support of finite element modeling.

3.2 Task 2 - Analysis

GT will analyze the proposed new mixed-mode specimen designs using boundary element software in place at Georgia Tech (FRANC3D) prior to testing. These numerical results will be used to select conditions for a test matrix that is likely to reveal any crack growth mode transition.

GT will utilize post-test quantitative fractography data from Task 1 to generate boundary element models of crack paths in tested specimens in FRANC3D. Results of boundary element analyses will be compared to existing Mode I / II combined loading crack path selection models to characterize the effect of Mode III loading. Modifications or alternatives to existing models will be assessed in an effort to account for generalized Mode I / II / III loading.

Georgia Tech will incorporate additional experimental data furnished by Pratt &

Whitney or a third party into analysis and modeling efforts if the data is provided early enough for the analysis to be completed within the 2006 contract work period.

4 Project Status

4.1 Task 1 - Mechanical Testing

Due to manufacturing issues, Pratt & Whitney has not yet delivered an adequate number of titanium specimens that are suitable for testing. Specimens were originally planned to be received by Summer 2006. Work is currently underway to complete specimen fabrication at Pratt & Whitney within required tolerances. The possibility of reworking specimens already fabricated that cannot be tested in their current condition is being examined. GT and Pratt & Whitney have developed a design for new tooling that will allow previously fabricated but test-unsuitable specimens to be tested in existing fixtures. Strain gages and sample preparation materials for the titanium specimens have been acquired.

While titanium specimens were being fabricated, additional material (PMMA) was acquired to fabricate a number of surrogate specimens for use in specimen validation. The crack growth and crack path selection behavior of PMMA is well

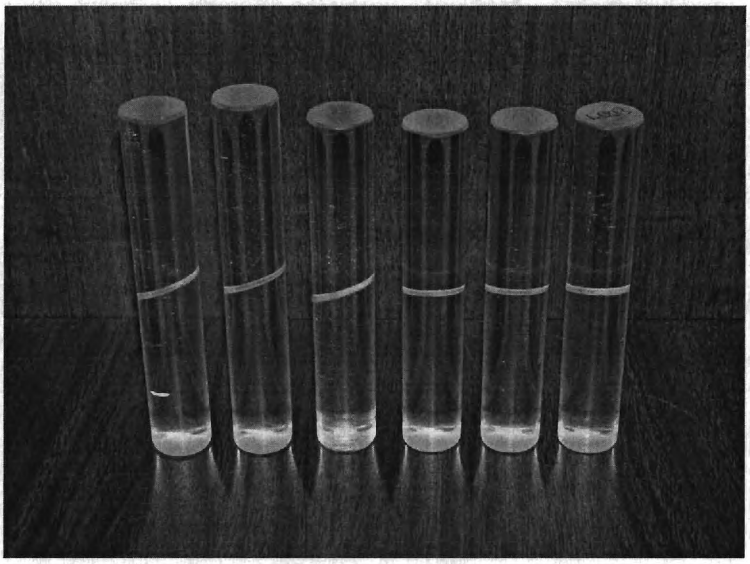

Figure 4.1: Initial surrogate PMMA specimens to be used for model validation.

understood and can be predicted with good accuracy. Testing one of the new specimen designs using PMMA will allow GT to validate the results of the finite element (FE) models of the specimen that have been developed prior to application of the FE model results to the titanium specimens. Several PMMA specimens of the second specimen design, shown in Fig. 4.1, have been fabricated at two different initial flaw angles and are ready for initial validation testing.

4.2 Task 2 - Analysis

Numerical modeling of the two new specimen designs in their initial pre-cracked configurations is complete, and closed-form solutions for the stress intensity factors required for test matrix generation are available. The methodology and results of the analyses is described below.

4.2.1 Specimen geometries

Inclined circumferential crack specimen

The first specimen design is a variation on the common circumferentially notched cylindrical specimen used in Mode I and III crack growth studies. The inclined circumferential crack (ICC) specimen, shown in Fig. 4.2, consists of a solid round bar with a circumferential slot of length a inclined at an angle β to the normal load plane. The inclined angle of the pre-flaw produces coupled Mode I and II stress intensities under tensile loading, with the mode mixity being a function of β, and Mode III loading is generated by an applied longitudinal torque. This specimen produces a single stress state all along the crack front for focused studies of specific stress intensity mixities. In order to generate as sharp a crack-like pre-flaw as possible, this specimen must be slotted with electro-discharge machining (EDM) using a thin, inclined electrode while the specimen is rotated on a chuck about its axis, and thus

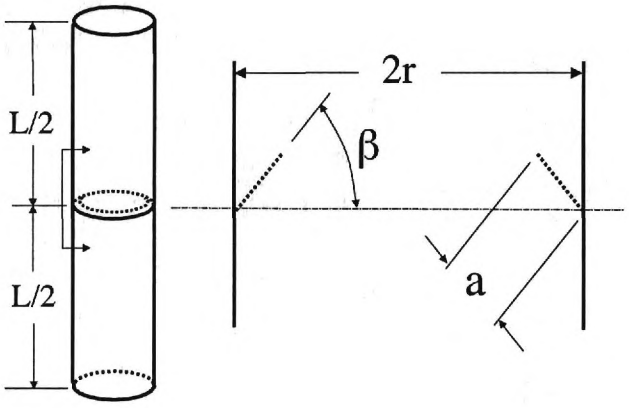

Figure 4.2: Sketch of inclined circumferential crack (ICC) specimen configuration and dimensions.

is not suitable for some non-conductive materials.

Inclined through-crack specimen

The second design, the inclined through-crack round (ITCR) specimen, consists of a solid round bar with a narrow internal slit passing through the center of the specimen inclined at an angle β to the normal load plane, as shown in Fig. 4.3. An applied tensile load produces coupled Modes I and III loading with a mixity as a function of β that is relatively constant all along the two crack fronts. A longitudinal torque produces a radial (and nearly linear) distribution of Mode II loading, from zero at the crack front midpoint to maxima at the extremities. This specimen generates a distribution of effective stress intensity factor and mode mixities in order to allow exploration of stress states that may result in a modal transition in crack growth.

A previous approach to generating 3-D mode mixities for fracture testing utilized a three-point bend specimen with an inclined crack [16]. An advantage to this

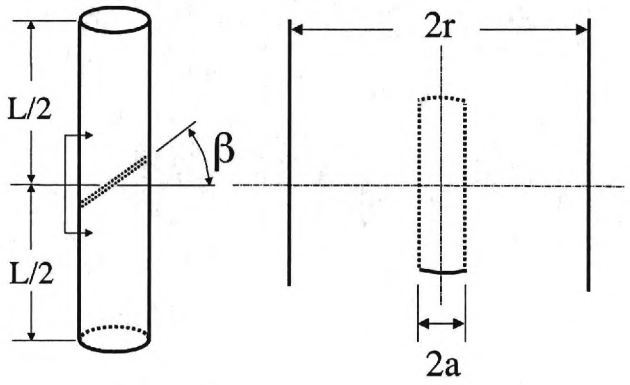

Figure 4.3: Sketch of inclined through-crack round (ITCR) specimen configuration and dimensions.

approach through the use of a tension-torsion specimen configuration is that one of the shear modes can be controlled independently of the other two modes, so that a wide range of out-of-phase loads may be applied for isolated study of one of the shear modes. For example, a constant Mode III crack load can be superimposed on coupled, cyclic Mode I/II loads using the ICC specimen to investigate alterations to traditional 2-D crack path prediction criteria. In the ITCR specimen, a cyclic torque can be used to apply a range of ΔK_{II} across the crack front while the coupled K_I and K_{III} are held constant, or increased to their maxima out of phase with K_{II}.

4.2.2 Modeling approach

Geometry, material and boundary conditions

Stress intensity factors for the new specimen designs were numerically modeled using the OSM (Object Solid Modeler), FRANC3D (FRacture ANalysis Code for 3D) and BES (Boundary Element System) software packages available from the Cornell

Fracture Group. The analysis approach of FRANC3D treats the underlying topology (created using OSM) separately from the geometry of the boundary element mesh, and boundary conditions are applied directly to the topological surface patches independent of discretization. The underlying geometry for both specimens generated in OSM is a cylinder 76.2 mm in length and 19 mm in diameter, in which each end consists of four quarter-circular surface patches and the sides of the cylinder consist of eight extruded quarter-circular surface patches as shown in Fig. 4.4. The eight

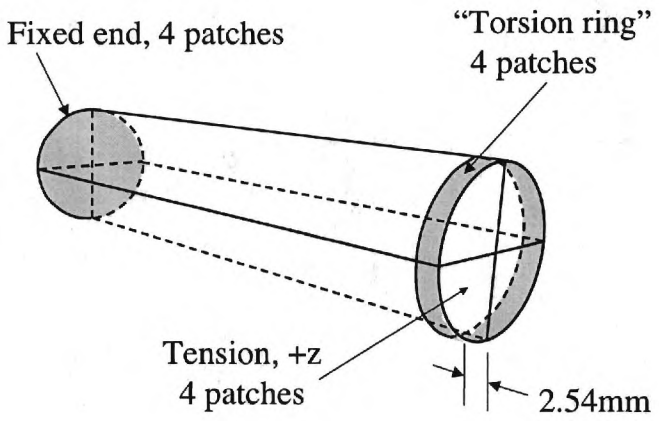

Figure 4.4: Underlying OSM geometry for BEM analysis showing discrete ring of surface patches for applications of torque.

surface patches of the round sides of the cylinder were created by subdividing the sides lengthwise at 2.54 mm from one end of the specimen to form a small ring of surface patches at that end labeled "torsion ring" in Fig. 4.4. Since traction boundary conditions are applied to entire surface patches in FRANC3D, this isolated ring of surface patches was used for the localized application of a torsional load to represent conditions in a tension-torsion test frame.

Both specimens were assigned material properties in FRANC3D corresponding

to a common aerospace titanium alloy (Ti-6Al-4V): Young's modulus $E = 114$ GPa, Poisson's ratio $\nu = 0.34$. A surface traction of 1,249 MPa was applied to the four "torsion ring" patches in the tangential direction of the local coordinate system corresponding to a positive torque of 113 Nm along the z-axis of the specimen. The tensile load of 44 kN was applied by a normal traction in the positive global z-direction of 156 MPa. The four surface patches of the $z = 0$ end of the specimens were subject to fixed boundary conditions ($u_i = \theta_i = 0$, $i = x, y, z$). While this resulted in a local stress concentration at the end due to restriction of the Poisson contraction, these effects dissipated within several millimeters of the end and did not disturb the stress distribution near the cracks. Both specimens were modeled in the tension-torsion condition as well as the tension-only condition; results for torsion-only were obtained simply by the difference of the two load conditions.

ICC specimen models

The normal procedure for modeling cracked components in FRANC3D is to generate the uncracked component geometry in OSM and then insert the crack surface using subroutines within FRANC3D. For the ICC specimen, however, the surfaces of the conical circumferential crack in the ICC specimen had to be generated in OSM and designated as internal patches prior to importing into FRANC3D for successful modeling. Three crack angles and three crack lengths each were modeled: $\beta = 0°$, 30°, and 45°; and $a/r = 0.08$, 0.12, and 0.16. The crack surfaces were meshed with 4-node quadrilateral elements approximately 0.2 to 0.3 mm in size.[1] While there was considerable mesh refinement near the crack mouth on the specimen surface, the rest of the specimen mesh was fairly coarse, as shown in Fig. 4.5; however, a refinement study showed that roughly doubling the remote mesh density had a negligible impact

[1]In FRANC3D, element mid-side nodes are not explicitly specified during meshing, but are generated when writing the BES files for either a linear or quadratic analysis. All of the analyses herein were linear, so all of the elements default to 4-node quadrilaterals and 3-node triangles.

(less than 0.5%) on the stress intensity results.

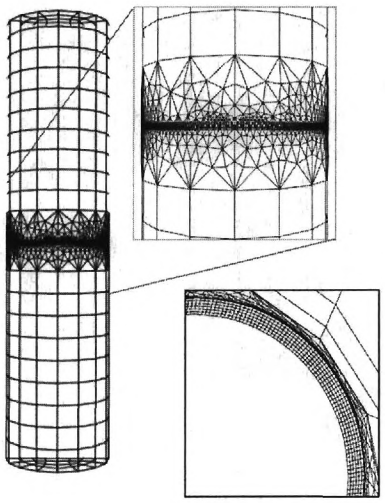

Figure 4.5: BEM mesh for ICC specimen, $\beta = 45°$, with gage section refinement and a section of internal crack surface mesh shown in insets.

ITCR specimen models

The ITCR specimen was also modeled with three crack angles and three crack lengths each: $\beta = 0°$, 30°, and 45°; and $a/r = 0.133$, 0.167, and 0.233. The crack surfaces were meshed with 4-node quadrilateral elements approximately 0.3 mm in size. A similar approach to mesh refinement only in the vicinity of the crack-free surface intercepts was employed as with the ICC specimen, as shown in Fig. 4.6 for all three crack angles. A full-specimen refinement study also showed a negligible impact of the remote mesh density on the crack tip stress intensity results.

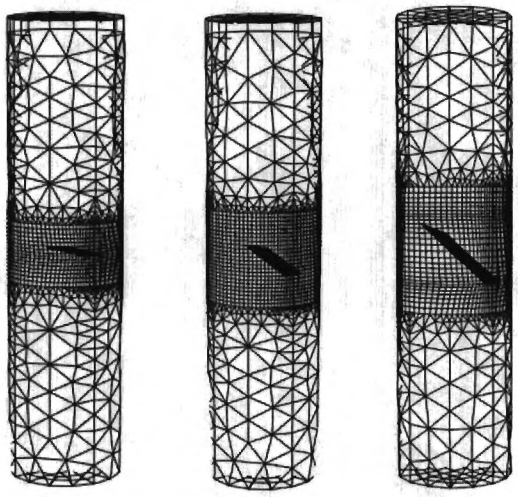

Figure 4.6: BEM meshes for ITCR specimens, $\beta = 0°$, 15°, and 30°.

4.2.3 Discussion of results

ICC stress intensity solution

Curve-fit equations for the stress intensity factors developed from the 18 load cases simulated are presented below:

$$\begin{aligned} \mathrm{K_I} &= \sigma_o\sqrt{\pi a}\,(\cos\beta + 0.555\cos^2\beta)\left(0.653 + 0.401\tfrac{a}{r}\right) \\ \mathrm{K_{II}} &= 0.394\sigma_o\sqrt{\pi a}\sqrt{\sin\beta} \\ \mathrm{K_{III}} &= \tau_o\sqrt{\pi a}\,(\cos\beta - 0.088\cos^2\beta)\left(0.962 + 1.544\tfrac{a}{r}\right) \end{aligned}$$

where $\sigma_o = P/\pi r^2$ and $\tau_o = 2T/\pi r^3$. It should be noted that this stress intensity solution differs slightly from the approach taken in the commonly used circumferential crack solution in the handbook by Tada *et al.*[17]. In that standard ($\beta = 0$) solution, the reference stresses σ_n and τ_n are net section stresses at the minimum radius, and for the case of torsion-induced $\mathrm{K_{III}}$ is not presented directly in terms of

crack length as herein. In this solution, the full crack length a is measured along the inclined plane as described above, and the reference stresses σ_o and τ_o are based on the uncracked section radius r.

Comparison of the fitting equations to the BEM data for the nine simulations at P = 44 kN and T = 113 Nm is shown in Fig. 4.7. The average of the absolute value

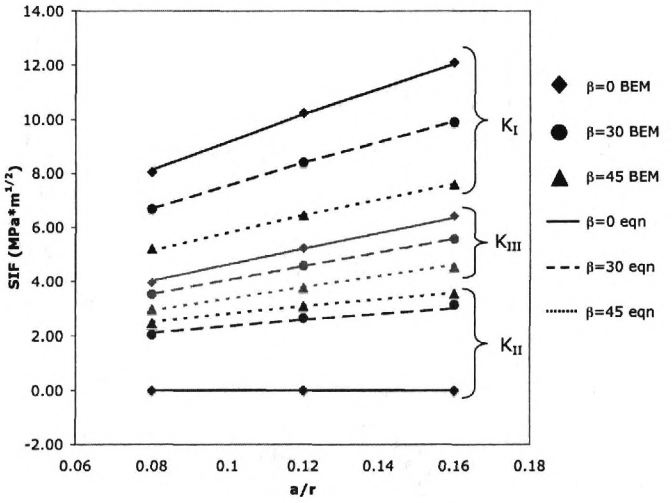

Figure 4.7: Comparison of closed-form stress intensity solution with BEM results for the ICC specimen.

error for all 18 cases is 1%, with a maximum error of 4.3% for the $\beta = 45°$, $a/r = 0.08$ case.

For the purpose of investigating crack path selection and the possibility of modal transition to shear crack growth, this specimen is capable of generating a Mode I/II mixity as low as $M_e = 0.71$ for $\beta = 45°$, where

$$M_e = \tan^{-1}\left(\frac{\mathrm{K_I}}{\mathrm{K_{II}}}\right).$$

This is not a low enough mixity to reproduce the modal transition results previously

observed in the studies cited above (in which M_e values as high as 0.56 led to shear crack growth mode). However, the Mode III component of loading is independently controlled by the torque applied to the specimen, and in the load case modeled in this study (σ_o = 156 MPa and τ_o = 83 MPa), the amount of K_{III} produced was 20-28% higher than K_{II} over the range of a/r investigated, substantially increasing the shear loading on the crack tip. This specimen may therefore be used, for example, to study the influence of K_{III} on the 2-D mode mixity M_e at which modal transition may be observed in some materials.

ITCR stress intensity solution

An example of the stress intensity distribution across the two crack fronts of the ITCR specimen are shown in Fig. 4.8 for the case of P = 44 kN and T = 113 Nm, $a/r = 0.133$ and $\beta = 30°$. While the primary result of the torsional loading manifests

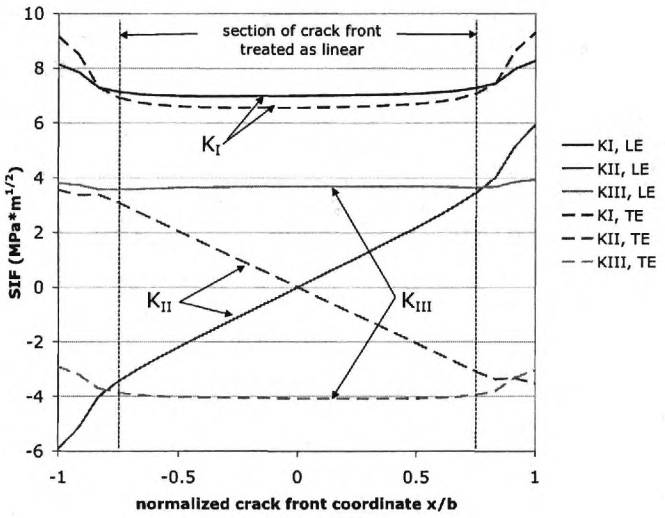

Figure 4.8: BEM stress intensity results for the ITCR specimen $\beta = 30°$, a = 1.25 mm, r = 9.5 mm under P = 44 kN and T = 113 Nm. Solid lines represent the "leading edge" crack front, dashed lines the "trailing edge."

as K_{II}, it can be observed that upon application of a torque to an inclined crack ($\beta >$

0), the stresses in the circumferential direction (specimen coordinate system) produce stress components in the normal and out-of-plane shear directions when transformed to the crack tip coordinate system. This results in contributions to K_I and K_{III} from the torque that are additive on one crack front (named herein the "leading edge" crack front, shown by solid lines in Fig. 4.8) and subtractive on the other (named the "trailing edge," shown by dashed lines). As with the ICC specimen, the ITCR specimen can produce significant proportions of K_{III} to augment the crack tip shear stresses of the torque-induced K_{II}, though in this case K_{III} is coupled with K_I as a function of β. Additionally, the ITCR specimen is capable of significantly higher proportions of K_{II} across the crack front than the previous three-point bend approach mentioned above (both the $\gamma = 45°$ inclined crack in three-point bending configuration and the $\gamma = 90°$ normal crack in out-of-plane shear configuration). The ITCR specimen can thus produce a wide range of mode 3-D mixities with significant levels of shear loading along a single crack front for the study of crack path deflection and crack growth mode.

In order to simplify the stress intensity curve fits for this specimen for the purpose of quickly selecting experimental loads and mode mixities, the stress intensity distributions were assumed to be nominally linear, even though there is some non-linearity in K values across the crack front, with significant deviations near the free surface intercepts. Along the innermost 75% of the crack front, demarcated in Fig. 4.8, the BEM data fall within a 5% error band of a linear fit. Therefore, the stress intensity equations for this specimen were determined based on the average value of K_I and K_{III}, or the slope of a linear fit for the values of K_{II}, over the range $-0.75 < x/b < 0.75$, where the crack front length $b = \sqrt{r^2 - a^2}$, and the free surface effect at the crack ends is neglected. The stress intensity equations determined by

this approach are

$$
\begin{aligned}
K_I = \quad & \sigma_o\sqrt{\pi a}\,\cos^2\beta\left(0.8162+0.8286\tfrac{a}{r}\right) \\
& \pm\,\tau_o\sqrt{\pi a}\,\sin\beta\cos\beta\left(-0.018+0.759\tfrac{a}{r}\right) \\
K_{II} = \quad & \tfrac{x}{b}\left[\tau_o\sqrt{\pi a}\,\cos\beta\left(0.7114+2.3439\tfrac{a}{r}-4.6816(\tfrac{a}{r})^2\right)\right] \\
K_{III} = \quad & \sigma_o\sqrt{\pi a}\,\sin\beta\cos\beta\left(0.8513+0.3933\tfrac{a}{r}\right) \\
& \pm\,\tau_o\sqrt{\pi a}\,\left(\sin^2\beta-\cos^2\beta\right)\left(-0.0199+0.6846\tfrac{a}{r}\right)
\end{aligned}
$$

where σ_o and τ_o are defined as above, and the x/b term indicates the radial distribution of K_{II} across the crack front. The $\pm$ symbol in equations for K_I and K_{III} indicates that the contribution of torque to Modes I and III is additive on the leading and trailing edges and subtractive on the trailing and leading edges, respectively.

Comparisons of the fitted equations to the BEM data are shown in Figs. 4.9 and 4.10 for two extrema of the simulated conditions for the r = 19 mm specimen model: $\beta = 0°$, $a/r = 0.133$; and $\beta = 30°$, $a/r = 0.233$. Both show excellent agreement between the curve-fits and the data, with the equations predicting within 5% of the BEM simulations in the $-0.75 < x/b < 0.75$ range. For further validation, two new models of $\beta = 30°$ specimens were developed using two different radii, r = 12.7 mm and r = 6.4 mm, while holding a constant $a/r = 0.133$. Both cases showed similar fidelity between the curve-fits and BEM data, as shown in Figs. 4.11 and 4.12. The highest error was seen in the prediction of K_{II} for the r = 6.4 mm specimen, which strayed up to 6% from the BEM data.

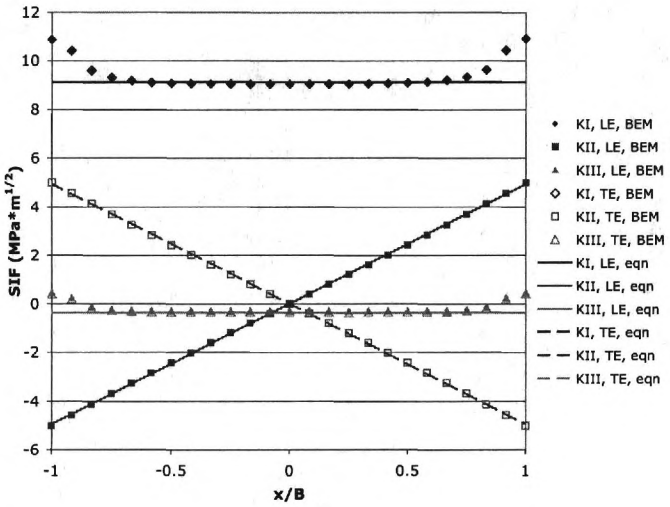

Figure 4.9: Comparison of closed-form stress intensity solution with BEM results for the ITCR specimen $\beta = 0°$, $a = 1.25$ mm, $r = 9.5$ mm under P = 44 kN and T = 113 Nm. Solid lines (curve fit) and closed symbols (BEM data) represent the "leading edge" crack front, dashed lines and open symbols the "trailing edge."

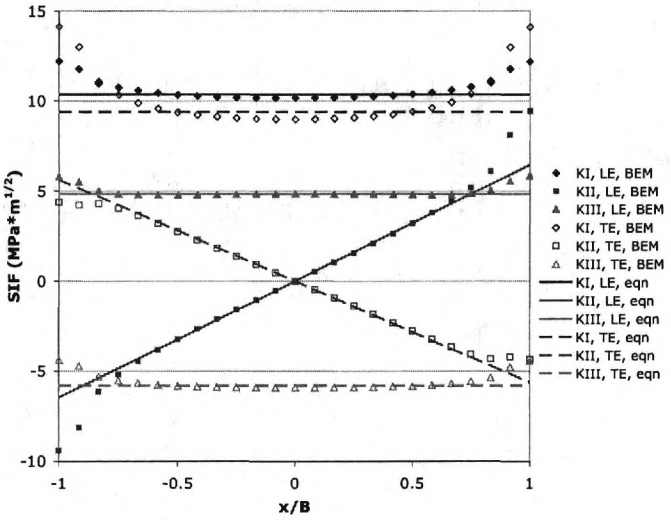

Figure 4.10: Comparison of closed-form stress intensity solution with BEM results for the ITCR specimen $\beta = 30°$, $a = 2.22$ mm, $r = 9.5$ mm under P = 44 kN and T = 113 Nm. Solid lines (curve fit) and closed symbols (BEM data) represent the "leading edge" crack front, dashed lines and open symbols the "trailing edge."

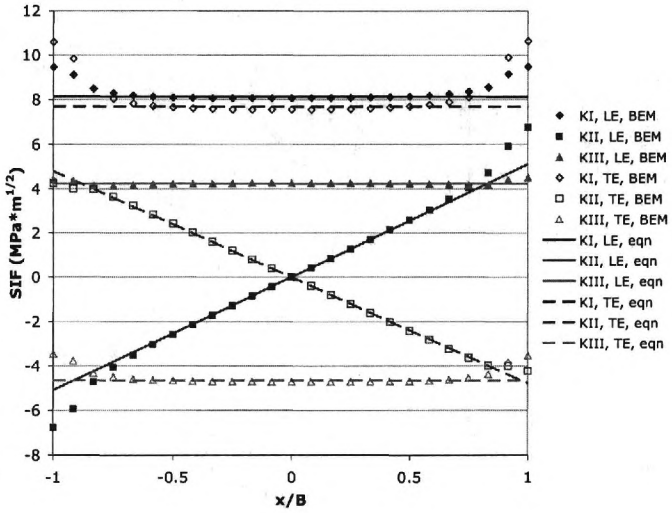

Figure 4.11: Comparison of closed-form stress intensity solution with BEM results for the ITCR specimen $\beta = 0°$, $a = 2.2$ mm, $r = 12.7$ mm under P = 78 kN and T = 268 Nm. Solid lines (curve fit) and closed symbols (BEM data) represent the "leading edge" crack front, dashed lines and open symbols the "trailing edge."

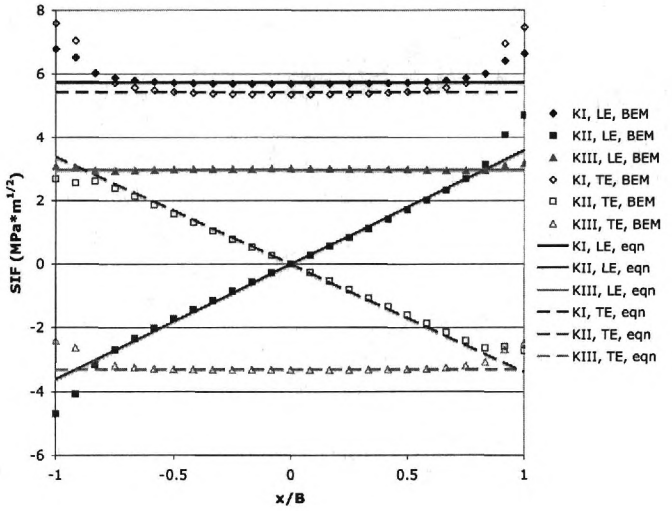

Figure 4.12: Comparison of closed-form stress intensity solution with BEM results for the ITCR specimen $\beta = 30°$, $a = 1.1$ mm, $r = 6.4$ mm under P = 19.6 kN and T = 33 Nm. Solid lines (curve fit) and closed symbols (BEM data) represent the "leading edge" crack front, dashed lines and open symbols the "trailing edge."

5 Future Work

5.1 Task 1 - Mechanical Testing

GT will perform tension-torsion fatigue crack growth tests on PMMA validation specimens in sufficient quantity and number of loading conditions to verify the accuracy of numerical models developed in the first contract year. At least two initial flaw angles will be tested to validate the modeled effect of crack angle.

GT will perform tension-torsion fatigue crack growth tests on up to thirty (30) titanium specimens total of up to three (3) design configurations, including the two designs already detailed herein. Tests will be conducted in such a manner as to generate combinations of Mode I, Mode II, and Mode III loading conditions and HCF/LCF interactions as specified by Pratt & Whitney. GT will record mechanical and/or electrical data as appropriate to monitor fatigue crack growth rate. The primary data deliverable from testing will be post-test quantitative fractography to characterize crack path direction in support of finite element modeling.

5.2 Task 2 - Analysis

GT will utilize quantitative fractography data from Task 1 to generate new FE models of final crack paths in tested specimens to calculate the stress conditions that dictate the favored crack paths. Results of finite element analyses will be compared to existing Mode I / II combined loading crack path selection models to characterize the effect of Mode III loading and validate the predictions of a new 3-D model. GT will attempt to develop a 3-D generalization of an existing 2-D crack path model, incorporating the MSS criterion, that should improve on existing 3-D crack path prediction methods, which rely only on the MTS criterion. GT will incorporate additional experimental data furnished by Pratt & Whitney or a third party into

analysis and modeling efforts if the data is provided early enough for the analysis to be completed within the extended contract work period.

6 Summary

Closed-form stress intensity solutions have been developed for two specimen configurations that have been analyzed and shown to generate significant levels of shear mode crack tip stress intensities in addition to normal Mode I stresses under tension-torsion loading. Both specimens can be used for investigations of the role of shear mode loading on crack path deflection and crack growth mode under 3-D mode mixities. The ICC specimen allows for study of the influence of Mode III loading on previously established 2-D mixed mode crack growth models through independently controlled torsional loading of the specimen. The ITCR specimen generates a range of Mode II loading across a crack front so that a transition point or critical mode mixity might be identified on a single fracture surface.

Surrogate PMMA specimens have been fabricated and are being prepared for specimen validation testing in early 2007. Efforts are underway to adapt or rework titanium specimens for subsequent material characterization testing, which will take place in Sprint 2007.

References

[1] F. Erdogan, G. Sih, On the crack extension in plates under plane loading and transverse shear, Journal of Basic Engineering 85D (4) (1963) 519–527.

[2] M. Hussain, S. Pu, J. Underwood, Strain energy release rate for a crack under combined mode I and mode II, in: Fracture Analysis, ASTM STP 560, ASTM, Philadelphia, 1974, pp. 2–28.

[3] G. C. Sih, Strain energy density factor applied to mixed mode crack problems, International Journal of Fracture 10 (1974) 305–321.

[4] M.-Y. He, J. W. Hutchinson, Kinking of a crack out of an interface, Journal of Applied Mechanics, Transactions ASME 56 (2) (1989) 270–278.

[5] D.-C. Tian, D.-Q. Lu, J.-J. Zhu, Crack propagation under combined stresses in three-dimensional medium, Engineering Fracture Mechanics 16 (1) (1982) 5–17.

[6] M. Schollmann, H. A. Richard, G. Kullmer, M. Fulland, A new criterion for the prediction of crack development in multiaxially loaded structures, International Journal of Fracture 117 (2) (2002) 129–41.

[7] J. Qian, A. Fatemi, Mixed mode fatigue crack growth: a literature survey, Engineering Fracture Mechanics 55 (6) (1996) 969–990.

[8] H. A. Richard, M. Kuna, Theoretical and experimental study of superimposed fracture modes I, II and III, Engineering Fracture Mechanics 35 (6) (1990) 949–960.

[9] J. C. W. Davenport, D. J. Smith, A study of superimposed fracture modes I, II and III on PMMA, Fatigue & Fracture of Engineering Materials & Structures 16 (10) (1993) 1125–33.

[10] L. P. Pook, On fatigue crack paths, International Journal of Fatigue 17 (1) (1995) 5–13.

[11] D. Hull, The effect of mixed mode I/III on crack evolution in brittle solids, International Journal of Fracture 70 (1) (1994) 59–79.

[12] F. G. Buchholz, V. Just, H. A. Richard, Computational simulation and experimental results on 3D crack growth in a 3PB-specimen with an inclined crack plane, in: F. G. Buchholz, H. A. Richard, M. H. Aliabadi (Eds.), Advances in Fracture Mechanics, Trans Tech Publications, Zurich, 2003, pp. 85–90.

[13] N. Hallback, F. Nilsson, Mixed-mode I/II fracture behavior of an aluminum alloy, Journal of Mechanics and Physics of Solids 42 (9) (1994) 1345–1374.

[14] B. E. Amstutz, M. A. Sutton, D. S. Dawicke, M. L. Boone, Effects of mixed mode I/II loading and grain orientation on crack initiation and stable tearing in 2024-T3 aluminum, in: R. Piascik, J. Newman, N. Dowling (Eds.), Fracture Mechanics: 27th Volume, ASTM STP 1296, Vol. 27 of ASTM STP 1296, American Society for Testing and Materials, 1997, pp. 105–125.

[15] Y. J. Chao, S. Liu, On the failure of cracks under mixed-mode loads, International Journal of Fracture 87 (1997) 201–223.

[16] F. G. Buchholz, A. Chergui, H. Richard, Fracture analyses and experimental results of crack growth under general mixed mode loading conditions, Engineering Fracture Mechanics 71 (4-6) (2004) 455–468.

[17] H. Tada, P. C. Paris, G. R. Irwin, Stress Analysis of Cracks Handbook, Del Research Corporation, Hellertown, PA, 2000.